

Infrared spectroscopy of Nova Cassiopeiae 1993 (V705 Cas) – IV. A closer look at the dust

A. Evans^{1*}, V. H. Tyne¹, O. Smith¹, T. R. Geballe², J. M. C. Rawlings³,
S. P. S. Eyres⁴

¹ *Astrophysics Group, School of Chemistry & Physics, Keele University, Keele, Staffordshire, ST5 5BG*

² *Gemini Observatory, 670 N. A’ohoku Place, Hilo, HI 96720, USA*

³ *Department of Physics and Astronomy, University College London, Gower Street, London, WC1E 6BT*

⁴ *Centre for Astrophysics, University of Central Lancashire, Preston, PR1 2HE, UK*

Version of 26 March 2005; ME1022rv.tex

ABSTRACT

Nova Cassiopeiae 1993 (V705 Cas) was an archetypical dust-forming nova. It displayed a deep minimum in the visual light curve, and spectroscopic evidence for carbon, hydrocarbon and silicate dust. We report the results of fitting the infrared spectral energy distribution with the DUSTY code, which we use to determine the properties and geometry of the emitting dust. The emission is well described as originating in a thin shell whose dust has a carbon:silicate ratio of 2:1 by number ($\sim 1.26:1$ by mass) and a relatively flat size distribution. The $9.7\ \mu\text{m}$ and $18\ \mu\text{m}$ silicate features are consistent with freshly-condensed dust and, while the lower limit to the grain size distribution is not well constrained, the largest grains have dimensions $\sim 0.06\ \mu\text{m}$; unless the grains in V705 Cas were anomalously small, the sizes of grains produced in nova eruptions may previously have been overestimated in novae with optically thick dust shells. Laboratory work by Grishko & Duley may provide clues to the apparently unique nature of nova UIR features.

Key words: circumstellar matter – stars: individual: V705 Cas – novae: cataclysmic variables – infrared: stars

1 INTRODUCTION

V705 Cas (1993) was a typical dust-forming nova which showed evidence for carbon, silicate and hydrocarbon dust (Evans et al. 1997, Mason et al. 1998). Early IUE observations (Shore et al. 1994) suggested that the grains grew to $\sim 0.2\ \mu\text{m}$ shortly after dust condensation. Mason et al. (1998) modelled broadband infrared (IR) data using a combination of dust types, and concluded that the circumstellar dust shell consisted of carbon and silicate grains in the ratio $\sim 8.5:1$ by mass.

Evans et al. (1997; hereafter Paper II) presented IR spectroscopy of the dust in V705 Cas, with some data covering the wavelength range $2\text{--}24\ \mu\text{m}$. In addition to nebular and coronal features, emission features normally associated with hydrocarbons – the so-called ‘Unidentified Infrared’ (UIR) bands – were present in the spectra. The UIR features in V705 Cas were at wavelengths 3.28 , 3.4 , 8.1 , 8.7 and $11.4\ \mu\text{m}$; the ‘8.1’ and ‘11.4’ feature seem to correspond respectively to the UIR features normally seen at $7.7\ \mu\text{m}$ and

$11.25\ \mu\text{m}$ (but see §4.6.2 below), while the ‘3.4’ feature was much stronger relative to the ‘3.28’ than is generally the case in other astrophysical environments. The properties of the UIR bands in V705 Cas and in other novae indicate a set of UIR features peculiar to novae (Geballe 1997), due either to the nova-specific environment or excitation conditions.

The $10\ \mu\text{m}$ spectrum of V705 Cas also displayed a prominent silicate feature at $\sim 10\ \mu\text{m}$ and possibly a broad, weak feature at $18\ \mu\text{m}$ (Paper II). The $10\ \mu\text{m}$ feature in V705 Cas was narrow, and peaked at $9.7\ \mu\text{m}$, in contrast to the broader silicate features in novae Aql 1982 and Her 1991, which were also shifted to longer wavelength (see Smith et al. 1995). This implies that the silicate in novae Aql and Her displayed a degree of crystallinity, whereas that in V705 Cas was amorphous.

In Paper II we fitted a simple function of the form $\nu^\beta B(\nu, T)$, where B is the Planck function at temperature T and β ($\simeq 1$) is a constant (the so-called β -index for the dust), to IR spectra in the range $2\text{--}24\ \mu\text{m}$, and concluded that the grains eventually grew to $\sim 0.7\ \mu\text{m}$. However, given the high quality of the data and the availability of the DUSTY code – which solves the radiative transfer in a dusty environment for a variety of conditions (Ivezić & Elitzur 1997,

* Contact for correspondence. Email address ae@astro.keele.ac.uk

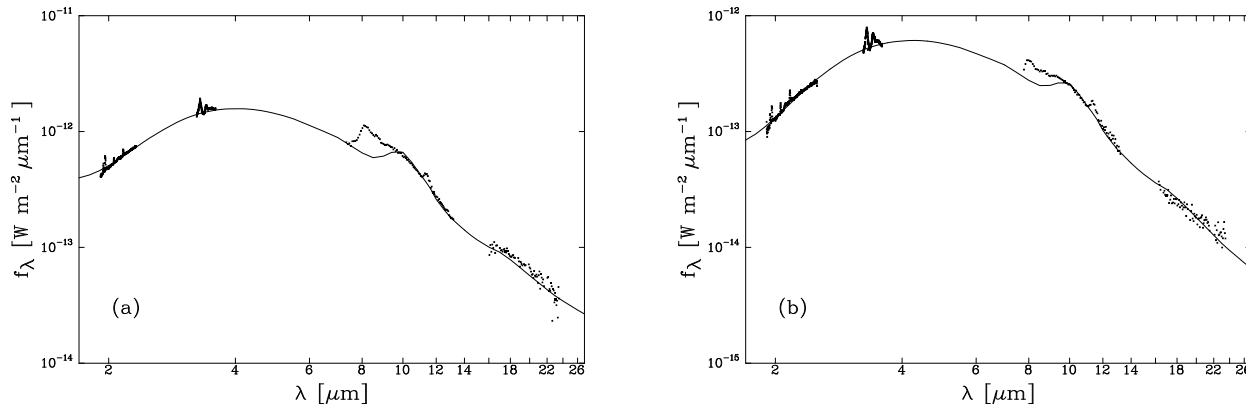


Figure 1. (a) Fit of DUSTY model to 1994 August data for nova V705 Cas; thick curve is DUSTY model. Note the strong UIR features in the $10\ \mu\text{m}$ window; the apparent ‘noise’ in the $\sim 2\ \mu\text{m}$ window is caused by the nebular lines. (b) As (a) but for 1994 October/November data.

Ivezić, Nenkova & Elitzur 1999) – we are now in a position to make a more sophisticated attempt at fitting the data and to re-evaluate the nature of the dust.

Here we describe the application of DUSTY to model the dust around V705 Cas.

2 THE DATA

The data analysed here are described in detail in Paper II; for consistency with earlier work we take reddening $E(B - V) = 0.5$ (Hauschildt et al. 1994) and 1993 December 14 as the origin of time. We revisit the distance below.

The fitting procedure works best if there are data on either side of the peak of the dust emission. For V705 Cas, two datasets satisfy this criterion, namely those for 1994 August (to which we shall refer as Epoch 1), and 1994 October/November (Epoch 2); at these two epochs we have quasi-simultaneous data over the wavelength range $2\text{--}4\ \mu\text{m}$ (K, L), $7.5\text{--}13\ \mu\text{m}$ (N), $16\text{--}24\ \mu\text{m}$ (Q), at resolution $\sim 300\text{--}1000$ (K, L bands) and ~ 60 (N, Q bands). The Epoch 1 data were obtained within 4 days of each other (on days 251 and 255 of the outburst, from Paper II; we take $t = 253$ days), while the Epoch 2 data were obtained within 40 days of each other (days 300 and 341; we take $t = 320$ days). The data are shown in Fig. 1.

In each case we assume that the nova and its environment did not change substantially between the times the data were obtained. Obviously this assumption is less secure for the October/November data but our attempts in Paper II to fit the data with the simple function as discussed above suggest that this assumption is not unreasonable.

3 THE FITTING

3.1 The state of V705 Cas in 1994

3.1.1 Preamble

We use observations of V705 Cas to estimate the likely properties of the nova and its environment at the time of our observations. For the purposes of the DUSTY fitting we shall

simply assume that the stellar remnant radiates like a blackbody. While more sophisticated models of the nova photosphere are now routinely available (see Hauschildt et al. 2002 and references therein), we have no *a priori* information about the state of ionization of the ejecta; however we expect that they are transparent to photons in the Lyman continuum at the times of interest.

The effective temperature T_* of a nova radiating at constant bolometric luminosity rises as the pseudophotosphere collapses back onto the white dwarf (Bath & Shaviv 1976). Consequently the emission shifts to shorter wavelengths and the visual flux (in mag) declines according to

$$|\Delta m_{\text{vis}}| \simeq 7.5 \log_{10} \left(\frac{T_*}{T_0} \right), \quad (1)$$

where Δm_{vis} is the decline in mag from maximum light and $T_0 \simeq 15,280\ \text{K}$ (Bath & Shaviv 1976). However, observational evidence is that novae at maximum are on the whole rather cooler than $15,280\ \text{K}$, a value closer to $\simeq 8,000\ \text{K}$ being more typical (Beck et al., 1995; Warner 1995); indeed the lower value is very close to the effective temperature determined for V705 Cas around maximum by Hauschildt et al. (1994). We take $T_0 = 8,000\ \text{K}$ here and use Equation (1) to estimate T_* .

We have taken the light curve in Paper II (reproduced in Fig. 2a) and determined \dot{m}_{vis} by a least squares fit over the period $t = 0$ days to $t = 60$ days, omitting ‘glitches’ such as the small pre-dust ‘dip’ noted in Paper II. We find

$$m_{\text{vis}} = 6.32(\pm 0.04) + 0.0364(\pm 0.0012) t, \quad (2)$$

where t is in days; we therefore have that $\dot{m}_{\text{vis}} = 0.0364 \pm 0.0012\ \text{mag day}^{-1}$ ($t_3 = 82.4 \pm 2.7$ days, $t_2 = 55.0 \pm 3.6$ days, t_n being the time for the visual light curve to decline by n mag), which differs somewhat from that assumed in Paper II ($\dot{m}_{\text{vis}} = 0.044\ \text{mag day}^{-1}$, $t_3 \simeq 68$ days) and is more in line with that given by Mason et al. (1998). We take $t_3 = 82.4$ days here.

Using the usual relationship between absolute magnitude and rate of decline (Della Valle & Livio 1995), the absolute visual magnitude of V705 Cas is $M_V = -7.05$ at maximum light; using a bolometric correction corresponding to an $8,000\ \text{K}$ supergiant the corresponding bolometric

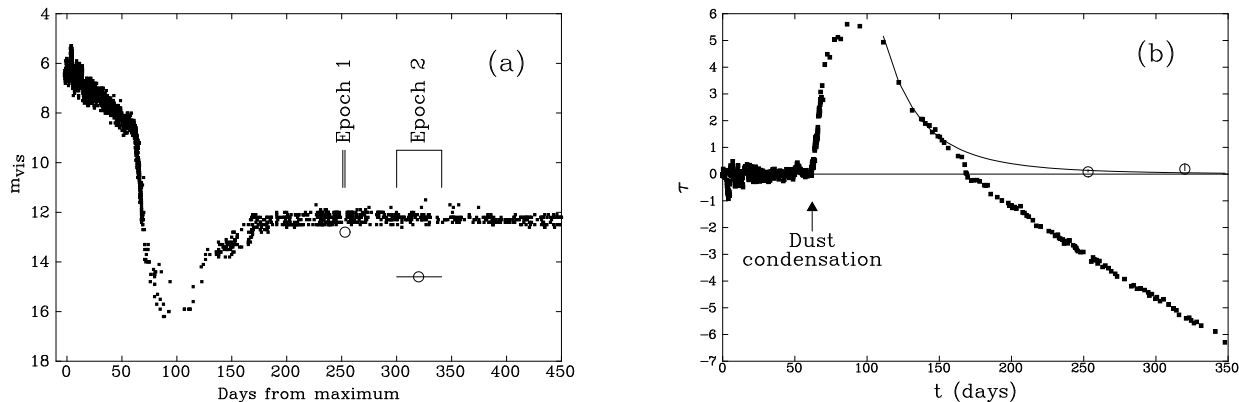


Figure 2. (a) Visual light curve of V705 Cas (filled squares), with Epochs 1 and 2 indicated; open circles are estimated location of pseudophotospheric continuum, based on DUSTY fits and after applying interstellar extinction corresponding to $E(B - V) = 0.5$. (b) Time-dependence of the optical depth in the dust shell during light curve recovery, estimated as described in text. This is effectively the visual light curve of V705 Cas but rectified by Equation (2), which is represented by the horizontal line. The curve is an estimate of the dust optical depth after the deep minimum; open circles are values of τ from DUSTY fits. See text for details.

luminosity is $5.6 \times 10^4 L_{\odot}$. The value of M_V , together with the value of $m_{\text{vis}}(t = 0)$ from Equation (2) and the assumed reddening, gives a distance of $D = 2.3 \pm 0.4$ kpc (cf. 3 kpc assumed in Paper II), in which the uncertainty in the reddening is the major contributor to the error.

3.1.2 Effective temperature of the remnant

We estimate the effective temperature of the stellar remnant using Equation (1). For Epoch 1, we find $T_* \simeq 135,000$ K, while for Epoch 2, $T_* \simeq 285,000$ K; there is a $\sim 10\%$ uncertainty in T_* that follows from the uncertainty in the coefficient of t in Equation (2). Although there are in principle several ways of corroborating these values, complementary data at other wavelengths are generally lacking.

In Paper II we noted the presence of [Si VI] ($^2P_{1/2} - ^2P_{3/2}$) at $\lambda = 1.963 \mu\text{m}$, which was fairly strong at Epoch 1 and also present at Epoch 2 ([Si VII] at $\lambda = 2.48 \mu\text{m}$ was also present, but very weak, at Epoch 2). The ionization potential of Si^{4+} is ~ 167 eV. If we assume that the gas is photoionized rather than collisionally ionized (see Benjamin & Dinerstein (1990) and Evans et al. (2003) for a discussion of this), the presence of the [Si VI] feature implies a sufficient number of photons with energy ≥ 167 eV. For strong [Si VI] emission we suppose for the purpose of estimate that half the emitted photons should be capable of ionizing Si^{4+} , implying an effective temperature $T_* \simeq 1.93 \times 10^6$ K. At $T_* \simeq 285,000$ K, only $\sim 2\%$ of the emitted photons are capable of ionizing Si^{4+} . The presence of the [Si VI] coronal line therefore seems to imply a T_* that is very much greater than 285,000 K; alternatively, a different ionization mechanism may be operating.

On the other hand, Orio, Covington & Ögelman (2001) have looked at *ROSAT* data for over 100 classical and recurrent novae. Although V705 Cas is not included in their discussion, they conclude that the ‘super-soft x-ray’ phase of the nova outburst is relatively short-lived, and is observed for only $\sim 20\%$ of novae: hot post-nova white dwarfs are relatively rare. Orio et al. hence estimate a general 1σ upper limit $T_* < 300,000$ K; the x-ray evidence (such as it is)

seems to point to a value of T_* consistent with that implied by Equation (1), and somewhat lower than that implied by the coronal lines.

In our preliminary investigations (Evans et al. 2002) we approximated the star by a blackbody with $T_* = 70,000$ K, and noted that the model IR spectrum is not sensitive to the temperature of the central object. However the predicted flux at $\lambda = 0.55 \mu\text{m}$ must not, after allowing for interstellar extinction, exceed the value implied by the visual light curve. This requires that the m_{vis} as calculated by DUSTY must be $\gtrsim 11$, which provides a further constraint on T_* .

3.1.3 Dust shell thickness and optical depth

CO was present in the IR spectrum of V705 Cas before maximum (Evans et al. 1996, hereafter Paper I). In Paper I we assumed that the relative thickness of the CO-bearing shell, $\Delta R/R$ (where R is the inner shell radius), was ~ 0.1 in V705 Cas. Furthermore consideration of the dust-forming potential of novae, together with the rapid recovery of the visual light curve after deep minimum, supports the view that the dust too is confined to a thin shell (Rawlings & Evans 2005). The value of $\Delta R/R$ for the dust shell is provided by our fitting procedure and, as the chemistry that leads to grain nucleation and grain formation is expected to be confined to the CO-bearing region, the DUSTY fitting may provide *a posteriori* justification for the assumption $\Delta R/R \sim 0.1$.

Dust precipitation began on day 62, after which the visual light curve went into deep decline. At this time, the difference between the *observed* visual magnitude and that predicted by Equation (1) is a measure of the visual optical depth τ of the dust shell; the time-dependence of τ is plotted in Fig. 2b. This is the visual light curve of Paper II, rectified by Equation (2), so that the visual decline described by Equation (2) is represented by the horizontal line. As the dust shell disperses (or breaks up) and the light curve recovers, the pseudophotospheric emission shifts to the ultraviolet (UV); at this time most of the visual light is provided by strong emission lines and Equation (1) no longer applies;

Table 1. Nova and dust shell parameters for V705 Cas for the two epochs. See text for discussion.

Property	Epoch 1	Epoch 2
t (days)	253	320
$F(\text{AC})$	$0.64^{+0.10}_{-0.04}$	$0.70^{+0.19}_{-0.07}$
$F(\text{Silicate})$	$0.36^{+0.10}_{-0.04}$	$0.30^{+0.19}_{-0.07}$
T_d (K)	604^{+3}_{-16}	612^{+12}_{-24}
a_{min} (μm)	$0.003 \pm 0.013^*$	$0.005 \pm 0.025^*$
a_{max} (μm)	$0.061 \pm 0.008^*$	$0.055 \pm 0.018^*$
q	$2.3 \pm 0.5^*$	$2.3 \pm 0.5^*$
R_{in} (cm)	$7.18^{+0.51}_{-0.58} \times 10^{15}$	$7.36^{+0.76}_{-1.37} \times 10^{15}$
θ_{in} (mas)	$417.3^{+29.6}_{-33.7}$	$427.8^{+44.2}_{-79.6}$
$1 + \Delta R/R$	$1.11 \pm 0.04^*$	$1.24 \pm 0.19^*$
τ	$0.085^{+0.082}_{-0.012}$	$0.19^{+0.20}_{-0.06}$
$f_{2.3}$ (10^{-10} W m $^{-2}$)	3.26	3.26
f_{dust} (10^{-12} W m $^{-2}$)	13.1	4.34
$f_{\text{dust}}/f_{2.3}$	0.040	0.013
T_* (K)	135,000	285,000
Estimated V_{phot}	12.8	14.8

for this reason the behaviour of the optical depth ‘data’ in Fig. 2b for $t \gtrsim 165$ days is not meaningful.

We see from Fig. 2 that maximum dust optical depth in the visual, $\tau_{\text{max}} \simeq 5.5$, was attained at $t \simeq 90$ days, and we estimate that the optical depth for Epoch 1 was ~ 0.1 , for Epoch 2 ~ 0.05 . The precise values are not important at this stage; however our fitting procedure determines the optical depth in the dust shell and our analysis of the data using DUSTY should produce values of this order.

3.1.4 Dust composition

The presence of the UIR hydrocarbon features is a strong indication that a form of carbonaceous dust is present. We therefore assume that the carbon component is amorphous carbon (AC), for which the optical constants are taken from Hanner (1988). As indicated above, there is also a silicate component, and we take optical constants for warm silicate from Ossenkopf, Henning & Mathis (1992).

We use our fitting procedure to determine the relative amounts of amorphous carbon and silicate dust in the shell.

3.2 Fitting the DUSTY models

For a given central source effective temperature, dust composition and dust shell properties, DUSTY calculates the ra-

diative transfer through a spherically symmetric dust shell and determines the observed spectral energy distribution (SED). DUSTY exploits the ‘scale-independence’ of the radiative transfer problem, so that the observed SED is effectively determined only by optical depth in the dust shell; this means that ‘absolute’ values (e.g. luminosity and dust shell dimensions) are not uniquely determined by the transfer problem and must be inferred by other means. We use a downhill simplex routine (see Press et al. 1992) to explore the multi-dimensional parameter space and to determine the best fit between the data and the DUSTY output (see Tyne et al. 2002 for details).

We assume an AC/warm silicate mix with a r^{-2} dust density distribution, appropriate for a steady wind. We optimize the fit by varying the carbon:silicate ratio, the dust temperature at the inner edge of the dust shell, the grain size distribution, and the geometric and (visual) optical thickness of the dust shell. Spectral features, namely the UIR features, and nebular and coronal lines, were removed before fitting the DUSTY output to the data, and restored once the fit had been optimized. The values of t , $f_{2.3}$ (the bolometric flux of the stellar remnant normalized to 2.3 kpc) and T_* for each epoch were fixed.

Further, as the relative placement of the spectra in the K , L , N and Q bands is uncertain by $\sim 10 - 20\%$ (a consequence of the uncertainty in the flux calibration), the relative placements of the individual spectral components were

adjusted in an iterative way to optimize the fit. For each *KLNQ* dataset, DUSTY was called typically about 50–60 times per optimization; including the iteration of the individual *KLNQ* bands, DUSTY ran some 300–400 times for each epoch to optimize the fit.

4 RESULTS & DISCUSSION

The best fits to the data for the two Epochs are shown in Fig. 1a,b; these are equivalent to Figure 3a,b of Paper II except that in the latter, there was no attempt to optimize the band-to-band fit (see §3.2), and the peak of the ‘8.1’ band was omitted. The best fit parameters are listed in Table 1, in which $F(\text{AC})$ and $F(\text{Silicate})$ are respectively the fractions (by number) of amorphous carbon and silicate grains in the dust shell; by definition, $F(\text{AC}) + F(\text{Silicate}) \equiv 1$. T_d is the dust temperature at the inner edge of the dust shell, a_{\min} and a_{\max} are the minimum and maximum grain size in the grain size distribution

$$n(a) da \propto a^{-q} da \quad (a_{\min} < a < a_{\max});$$

here a is grain radius, $n(a) da$ is the number of grains with radius $\in [a, a + da]$, and q is a constant.

In Table 1, f_{dust} is the power output from the dust shell (at 2.3 kpc), and τ is optical depth in the V band. For distance 2.3 kpc, the bolometric luminosity of the nova is $5.6 \times 10^4 L_{\odot}$ at both Epochs (see Table 1 and §3.1.1), a consequence of our assumption of constant bolometric luminosity (see Equation (1)).

The uncertainties in a given parameter were obtained by fixing all other parameters and varying the given parameter so as to increase the reduced χ^2 by unity on either side of the minimum; where this procedure failed to converge in a reasonable number of iterations and only one error bound was obtained, this error is used and is indicated by an asterisk in Table 1. The values of R_{in} follow from the input radiation field and fitted T_d (see Ivezić et al. 1999); the uncertainties in R_{in} are derived from the corresponding errors in θ_{in} .

Also given, in Table 1 and on Fig. 2, is the estimated contribution V_{phot} of the pseudophotosphere to the observed visual magnitude, based on the pseudophotospheric temperature, τ and interstellar extinction; the estimated values of V_{phot} clearly satisfy the requirement that they lie below the visual light curve (see §3.1.2).

4.1 The dust temperature

The dust temperature at the inner radius of the dust shell is determined to be $T_d = 604$ K at Epoch 1, and 612 K at Epoch 2, i.e. essentially constant between the two Epochs within the uncertainties. These values are comparable to those determined by Mason et al. (1998, their Figure 1), on the basis of fitting Planck functions to broadband data for $t \lesssim 275$ days. However if the central star delivers constant power input to the inner radius of the dust shell, which consists of a single grain type that is unchanging (so that the grain properties are also unchanging), we must have that

$$T_d = T_c \left(\frac{t_c}{t} \right)^{2/(\beta+4)}, \quad (3)$$

for a dust shell moving away from the site of the explosion at uniform speed; here T_c is the grain condensation temperature and t_c ($\simeq 62$ days; see Fig. 2a,b) is the condensation time. From Equation (3), we expect the value of $T_d t^{2/(\beta+4)}$ to be \simeq constant, whereas for V705 Cas it rises from $\sim 5524_{-146}^{+28}$ K day $^{0.4}$ (Epoch 1) to $\sim 6149_{-241}^{+121}$ K day $^{0.4}$ (Epoch 2), assuming $\beta = 1$ (the value assumed is not critical). This behaviour, in which the dust temperature does not decline in accord with Equation (3), is typical of dusty novae displaying ‘isothermal’ behaviour.

4.2 The optical and geometrical depth

The geometrical thickness of the dust shell, $\Delta R/R$, is $\simeq 0.11 \pm 0.04$ at Epoch 1, and $\simeq 0.24 \pm 0.19$ at Epoch 2 (see Table 1). In Paper I we assumed that the relative thickness of the CO-bearing shell, $\Delta R/R$ (where R is the inner shell radius), was ~ 0.1 in V705 Cas. While this choice was somewhat arbitrary it was governed by the fact that, in a nova wind that declines with time, there will be a thin dense shell at the outer edge of the ejecta (cf. Kwok 1983). Our DUSTY fitting indicates that the dust did indeed seem to have been confined to a thin ($\Delta R/R \sim 0.1$) shell at the outer edge of the ejecta. Indeed, the similarity of the dust temperatures at the inner shell determined here (see §4.1), and those determined by Mason et al. (1998) on the assumption of an isothermal dust shell, is a consequence of the fact that the dust shell is geometrically thin so that the isothermal approximation is a good one.

Very roughly, for an optically thin dust shell in which grains scatter isotropically, the ratio of the dust flux to the bolometric stellar flux is \sim the optical depth through the shell, suitably averaged over wavelength. However the carbon and silicate grains in V705 Cas do not scatter isotropically and so this relationship will only be approximately correct; nevertheless it is gratifying to see in Table 1 that $f_{\text{dust}}/f_{2.3} \sim \tau$.

4.3 Dimensions of the dust shell

The inner radius of the dust shell, R_{in} , is 7.18×10^{15} cm (7.36×10^{15} cm) at Epoch 1 (Epoch 2). At 2.3 kpc, the corresponding angular diameter θ of the inner edge of the dust shell is 417 mas (427 mas) at Epoch 1 (Epoch 2).

It is of interest to compare these values with the work of Diaz, Costa & Jatenco-Pereira (2001), who resolved the remnant of V705 Cas at $2.1 \mu\text{m}$ at $t = 2505$ days (relative to the time origin assumed here). They determined an angular diameter of 840 mas, and concluded that emission by the resolved remnant they observed could not be free-free, and that the SED of the remnant could be represented by a blackbody at 1100 K. This value led Diaz et al. to conclude emission by dust; however our results, as well as those of Mason et al. (1998), show that the dust temperature was as low as ~ 600 K at $t \simeq 250$ days, and it is difficult to see how the dust temperature could be elevated to 1100 K by $t = 2505$ days.

ISO observations of V705 Cas (Salama et al. 1999), at $t = 950, 1265$, and 1455 days, failed to detect any dust, with a limit of 0.3 Jy ($\sim 1.4 \times 10^{-13}$ W m $^{-2}$ μm^{-1}) at $\sim 2.5 \mu\text{m}$, the lower limit of the ISO SWS. The flux in the resolved

shell at $2.2\ \mu\text{m}$ was $4.1 \times 10^{-17}\ \text{W m}^{-2}\ \mu\text{m}^{-1}$ (Diaz et al. 2001) so on this basis we can not rule out the possibility that these authors detected the shell.

However if we and Diaz et al. have observed the same material, we would expect the angular diameter at Epoch 1 (Epoch 2) to be 85 mas (107 mas) for uniform expansion, significantly smaller than the ~ 420 mas implied by our DUSTY fitting. There are two likely reasons for this discrepancy: First, if the emission seen by Diaz et al. is in the form of emission lines (e.g. Pa- β $\lambda 1.28\ \mu\text{m}$, Br- γ $\lambda 2.16\ \mu\text{m}$), the J and K band fluxes would be elevated relative to H , as observed by Diaz et al. For example, in data obtained for our programme on 1996 August 22 ($t = 982$ days), the P β and Br γ fluxes are $1.7 \times 10^{-16}\ \text{W m}^{-2}$ and $3.2 \times 10^{-17}\ \text{W m}^{-2}$ respectively. Using the filter bandwidths for the system used by Diaz et al., together with their J and K -band fluxes for the extended shell, their in-band fluxes are $\sim 2.9 \times 10^{-17}\ \text{W m}^{-2}$ (J) and $\sim 1.4 \times 10^{-17}\ \text{W m}^{-2}$ (K) respectively. Given the difference in time between our 1996 August observation and that of Diaz et al., and the likely decline in the line fluxes between the observations, it seems plausible that they detected extended emission from recombination lines.

Second, with the T_d values from Table 1 and bolometric luminosity $L_* = 5.6 \times 10^4 L_\odot$, blackbody grains would lie at distance $\sim 7.5 \times 10^{14}$ cm from the stellar remnant, an order of magnitude smaller than the R_{in} values in Table 1. On the other hand, spherical graphitic grains of radius a_{max} and having the Planck mean absorption efficiency given by Gilman (1974) would be at $\sim 5 \times 10^{15}$ cm. The deduced R_{in} depends on both the nature of the grain material and (via the T_* -dependence of its Planck mean absorption efficiency) on T_* ; the situation is further complicated in the case of V705 Cas by the grain mix and by the relatively weak constraint on T_* (see § 3.1.2). This underlines the fact (see above) that the dust shell dimensions are not uniquely determined by the radiative transfer problem.

4.4 The grain size distribution

The grain size distribution $n(a) da \propto a^{-q} da$, with $q \simeq 2.3$, with no significant change in q between the two Epochs. In the environments of evolved stars, it is usual for the value of q to be $\gtrsim 3$, a value typical of grain-grain shattering (Hellyer 1970; Jones et al. 1995). The size distribution we have deduced for V705 Cas is significantly flatter than this. Such a situation may arise if grain growth/coagulation, destruction and shattering in the wind of V705 Cas competed in such a way that the larger grains survived at the expense of smaller, possibly as a result of the former sweeping up the latter. Given that the charging of grains in nova winds has a significant impact on the rate at which grains grow, coagulate and ablate (Shore & Gehrz 2004; Rawlings & Evans 2005), this is not unexpected; however we do not pursue this in detail here.

Evans & Rawlings (1994) have concluded that free-flying polycyclic aromatic hydrocarbon (PAH) molecules would not survive the harsh nova radiation field. The sizes of the smallest grains in the distribution are not well-constrained, so we can not confidently determine whether the UIR features arise in free-flying PAHs or from the vibration of C-H bonds on the surface of hydrogenated amorphous carbon (HAC) grains.

The maximum grain size, on the other hand, is rather better constrained. We find that the largest grain size is $\simeq 0.06\ \mu\text{m}$ at both Epochs. This is significantly smaller than deduced in Paper II ($\lesssim 0.54\ \mu\text{m}$ at Epoch 1, $\gtrsim 0.57\ \mu\text{m}$ at Epoch 2, and asymptotic dimensions $\sim 0.7\ \mu\text{m}$) on the basis of $\lambda^{-\beta} B(T, \lambda)$ fits to the data; such discrepancies are not unexpected given the simple-minded treatment in Paper II. However it is also significantly smaller than the $a \gtrsim 0.2\ \mu\text{m}$ (at $t = 65.5$ days) deduced – within days of dust precipitation – by Shore et al. (1994), on the basis of flat UV extinction shortward of $0.28\ \mu\text{m}$, and is substantially smaller than the grain size generally deduced in nova dust shells, $\sim 0.5 - 1\ \mu\text{m}$ (e.g. Gehrz et al. 1998). However we have performed several tests with large initial values of a_{max} and $a_{\text{max}} \simeq 0.06\ \mu\text{m}$ results irrespective of the starting value in the fitting routine, and we consider that this conclusion is robust.

We believe that the discrepancy between our a_{max} and that deduced by Shore et al. (1994) may have arisen, in part, for the following reason. Shore et al.'s conclusion was based on the fact that the UV extinction was neutral shortward of $\lambda \simeq 2800\ \text{\AA}$; they assumed that this implies $2\pi a/\lambda > 4$, so that $a > 0.18\ \mu\text{m}$. While this is valid for primarily scattering grains in the interstellar medium (see Spitzer 1978), it is less so for strongly absorbing (e.g. carbonaceous) grains in circumstellar environments, for which the condition for neutral extinction is closer to $2\pi a/\lambda > 1$. Indeed, the IR spectroscopic evidence is that the AC grains were the first to condense in the wind of V705 Cas (see §4.5), so the UV extinction seen by Shore et al. would have been due to AC rather than silicates. For V705 Cas therefore, the condition $2\pi a/\lambda > 1$ is likely the more appropriate, so that neutral extinction implies $a \gtrsim 0.045\ \mu\text{m}$. This would be more in line with the a_{max} values deduced here and would imply that, after an initial (~ 10 day) phase of very rapid increase in grain size, grain growth levelled off, possibly as the condensate was depleted.

More generally, grain size in nova winds is often deduced from

$$a = \frac{L_*}{16\pi\sigma T_d^4 R^2 (Q_e/a)} \phi(\tau_{\text{ext}}) \quad (4)$$

$$\simeq 1.87 \times 10^{22} \left[\frac{L_*}{L_\odot} \right] \left[\frac{V}{\text{km s}^{-1}} \right]^{-2} \left[\frac{t}{\text{days}} \right]^{-2} T_d^{-6} \mu\text{m}$$

(see Gehrz et al. 1980); this follows from equating the total power absorbed by the grains in the shell to the total re-radiated power. Here L_* is the (constant) bolometric luminosity of the stellar remnant, R is the grain-nova distance, Q_e is the Planck mean of the grain emissivity, τ_{ext} is the optical depth due to extinction in the dust shell and $\phi(\tau_{\text{ext}})$ is a factor that takes into account extinction within the shell (see below). Equation (4) assumes graphitic grains, for which $Q_e \propto a T_d^2$

Equation (4) with $\phi(\tau_{\text{ext}}) \equiv 1$ follows if (i) there is no internal extinction in the dust shell and (ii) the dust shell is geometrically thin so that the isothermal grain approximation applies. Application of Equation (4) to novae at IR maximum leads typically to grain sizes $\sim 1\ \mu\text{m}$, considerably larger than even the a_{max} deduced here. For example, in the case of V705 Cas, and taking relevant parameters from Mason et al. (1998), we find $a(\text{IR max}) \simeq 1.4\ \mu\text{m}$.

A possible explanation of course is that, as the a_{\max} deduced here is for $t > 253$ days, well after IR maximum (which occurred around $t \sim 100$ days in V705 Cas; Mason et al. 1998), there was a period of rapid grain destruction following the grain growth that preceded IR maximum. Indeed, application of Equation (4) to V705 Cas for times when τ_{ext} was small suggests that the grain radius initially increased, and eventually declined. Various scenarios for grain destruction have been proposed by Mitchell and co-workers (Mitchell, Evans & Bode 1983; Mitchell & Evans 1984; Mitchell, Evans & Albinson 1986) and it is inevitable that grains in nova winds are heavily processed (see Rawlings & Evans 2005).

Alternatively Equation (4) may not be appropriate at IR maximum for a dust shell that is *optically thick at short wavelengths*: as we have seen, assumption (ii) above is a good approximation in the case of V705 Cas but (i) is not. In this case,

$$\phi(\tau_{\text{ext}}) = \frac{1 - \exp[-\tau_{\text{ext}}]}{\tau_{\text{ext}}},$$

which $\rightarrow 1$ as $\tau_{\text{ext}} \rightarrow 0$. Applying this correction to V705 Cas at IR maximum gives $a(\text{IR max}) \simeq 0.2 \mu\text{m}$ for $\tau_{\text{ext}} \simeq 5.5$ (see §3.1.3), considerably less than that obtained on the assumption that the dust shell is optically thin.

We also note that Equation (4), with $\phi(\tau_{\text{ext}}) \equiv 1$, will apply whenever L_* is constant and the dust shell is optically thin at short wavelengths (as is the case after light curve recovery), as in V705 Cas at Epochs 1 and 2. Using $L_* = 5.6 \times 10^4 L_{\odot}$ from §4.2 and $V = 850 \text{ km s}^{-1}$, Equation (4) with $\phi(\tau_{\text{ext}}) = 1$ gives $0.5 \mu\text{m}$ ($0.3 \mu\text{m}$) at $t = 253$ days (320 days), again considerably smaller than that obtained for the time of IR maximum. While the situation in V705 Cas is complicated by the presence of (at least) two grain types, we conclude that the application of Equation (4) to determine grain size is inappropriate at infrared maximum in novae having optically thick dust shells.

4.5 The dust composition

We find that both sets of data are best fitted by a dust shell in which carbon grains are numerically more abundant than silicate grains. We do not expect the AC:silicate fraction to vary as the dust shell moves away from the stellar remnant, and the individual values of the AC and silicate fractions in Table 1 are gratifyingly constant; for the purpose of discussion we average the AC:silicate ratio, and integrate over the grain size distribution (see §4.4 below) to get a $\sim 0.67 : 0.33$ ($\pm \sim 0.1$) carbon:silicate mix. This translates to a mass ratio carbon:silicate = 1.26, significantly lower than the carbon:silicate ratio of ~ 8.5 obtained by Mason et al. (1998). However these authors fit a 4-component model to limited broadband data, with UIR components at their ‘standard’ wavelengths, and they caution that their derivation of the silicate mass may be problematic. We should not therefore be surprised by the discrepancy and consider that the result obtained here is reasonably robust.

The co-existence of carbon and silicate dust (‘chemical dichotomy’) in the IR spectra of evolved stars is usually ascribed to the trapping of silicate dust in a disc arising from mass-loss during an earlier phase of evolution when the star was oxygen-rich, while carbon dust arises from more recent

or current (carbon-rich) mass-loss (see e.g. Zijlstra et al. 2001 and references therein). In the case of V705 Cas, UIR emission was present in the $10 \mu\text{m}$ band when silicate was weak or absent (Evans et al. 1997). Novae may also have two well-separated mass-loss episodes with different chemistries to produce their chemical dichotomies, or there may be steep abundance gradients in the ejecta, or (as CO formation does not go to saturation; see Paper I, Pontefract & Rawlings 2004, Rawlings & Evans 2005) the nucleation chemistry allows the simultaneous formation of both carbon and silicate grains. In any of these cases, there may be interesting implications for the thermonuclear runaway, the nature of the nova explosion and the pre-dust chemistry.

While the assumptions leading to Equation (3) may not necessarily apply in the case of novae (see Evans & Rawlings 1994, Rawlings & Evans 2005 for a discussion of this), our values for the dust temperature at the inner edge of the shell imply condensation temperature $T_c \simeq 1060_{-28}^{+5}$ K (1153_{-46}^{+23} K) for Epoch 1 (Epoch 2); again the value of T_c is not sensitive to β and we have assumed $\beta = 1$. These values are of the right order for carbon condensation; however the situation in V705 Cas is complicated by the presence of two grain types, so the meaning of the ‘condensation temperature’ is not immediately obvious in this case. On the other hand, UIR emission and an underlying continuum, but no $9.7 \mu\text{m}$ silicate feature, were present in 1994 May (Paper II), implying that the AC condensed before the silicate.

4.6 The dust features

4.6.1 The silicate features

In Paper II we suggested that, in addition to the $9.7 \mu\text{m}$ silicate feature, there might also be present the corresponding $18 \mu\text{m}$ feature. The IR spectrum, together with the fitted model, in the range $7\text{--}25 \mu\text{m}$ for the two epochs is shown in Fig. 3; it seems that the $18 \mu\text{m}$ feature may indeed be present in the IR spectrum of V705 Cas, as may be seen by viewing Fig. 3 at grazing incidence.

As noted in Paper II, Nuth & Hecht (1990) suggested, on the basis of laboratory experiments on silicate analogues, that the strength of the $18 \mu\text{m}$ silicate feature relative to that of the $9.7 \mu\text{m}$ feature increases as the silicate ‘ages’ and is subjected to annealing. Processing of silicates, and its effect on the $9.7 \mu\text{m}$ feature in circumstellar environments, has been discussed from an observational point of view by Bouwman et al. (2001); however the objects (Herbig Ae/Be stars) in this study are young objects, and are not themselves dust producers and comparison with the silicates around evolved, dust-forming stars, is more relevant from our point of view.

To explore this we also include in Fig. 3 the ISO SWS spectrum of the actively dust-forming red supergiant μ Cep, which also displays prominent silicate features (see Tielens et al. 1997). We note in particular

- (i) the similarity of the $9.7 \mu\text{m}$ feature profiles in the two objects. The features are narrow, structureless, and peak around $9.7 \mu\text{m}$, suggestive of amorphous silicate;
- (ii) the relative strength of the $9.7 \mu\text{m}$ and $18 \mu\text{m}$ features, in that the ratio $18/9.7$ is much smaller in V705 Cas than

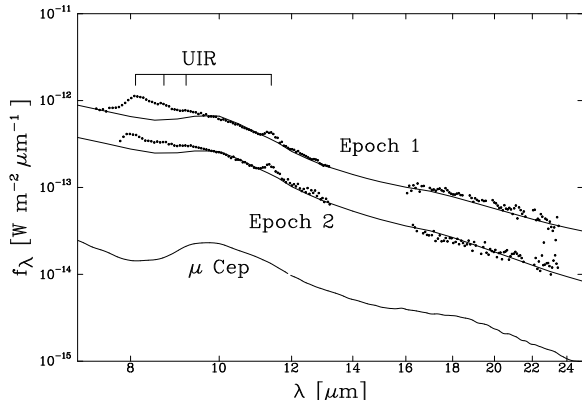


Figure 3. The profiles of the silicate features in V705 Cas for the two Epochs; the wavelengths of the 8.1, 8.6, 9.2 and 11.4 μm UIR features (see Fig. 4b and Table 2) are indicated. The curves through the data are the DUSTY fits; see text for details. Also shown for comparison (lower curve) is the ISO SWS spectrum of the red supergiant μ Cep.

in μ Cep, consistent with the view that the silicate in the nova is much ‘fresher’ than that in μ Cep.

While our data lend support to the conclusion of Nuth & Hecht (1990), the mid-IR spectra of novae, obtained over periods ranging from ~ 20 to ~ 1000 days from outburst (and hence over a range of annealing times), suggests that the situation is more complex than this. Although V705 Cas is now a very weak mid-IR source (the dust was not detected with the ISO SWS by Salama et al. 1999), further observations in the mid-IR (e.g. with the *Spitzer* Space Telescope (Werner et al. 2004)) will be valuable to monitor both the profile of the 9.7 μm feature – which may shift to longer wavelengths and display structure as the dust anneals – and the development of the relative strengths of the 9.7 μm and 18 μm features.

4.6.2 The UIR features

We have subtracted the model fit from the data in the *L* and *N* bands to reveal the profiles of the UIR emission (see Fig. 4a,b). Clearly the resultant UIR profiles in the *N* band depend to some extent on the profile of the warm silicate feature (Ossenkopf et al. 1992) but, as we are looking for possible changes in the UIR features this does not qualitatively affect the discussion that follows.

In Fig. 4a the *L*-band data from Epoch 2 data have been normalized to the Epoch 1 data at 3.4 μm and it is evident that, while the relative strengths of the 3.28 μm feature and the 3.5 μm ‘plateau’ are essentially unchanged between the two Epochs, the 3.4/3.28 ratio may have changed.

There is a weak feature at $\lambda = 3.522 \pm 0.001 \mu\text{m}$ (see Fig 4a). While this is close to the UIR feature at 3.52 μm (see Geballe 1997), the width of the feature in V705 Cas (FWHM $\sim 0.014 \mu\text{m}$ at Epoch 2 and corresponding to an expansion velocity $\sim 600 \text{ km s}^{-1}$) suggests that it might be a nebular feature rather than a dust feature, which would typically be much broader than this (see Table 2 below). Further IR spectroscopy of dusty novae in this spectral region is desirable to resolve this issue.

A possible (nebular) identification for this feature is H I 23-6 $\lambda 3.522 \mu\text{m}$, although there is no evidence for H I 24-6 $\lambda 3.501 \mu\text{m}$, which is expected to be of comparable strength. An alternative identification, particularly in view of the common occurrence of [Fe II] lines in the IR spectra of novae (Rudy et al. 2003; Evans et al. 2003), is [Fe II] $a^6\text{D}_{9/2} - a^4\text{F}_{5/2}$ at $\lambda = 3.52367 \mu\text{m}$. However there are many permitted and forbidden Fe II transitions in the wavelength range for which we have data and we defer a discussion of the emission line spectrum of V705 Cas to a later paper.

In Fig. 4b the *N*-band data from Epoch 2 data have been normalized to the Epoch 1 data at 9 μm ; the primary feature at $\sim 8.1 \mu\text{m}$ has a ‘shoulder’ at $\sim 8.6 \mu\text{m}$ and $\sim 9.2 \mu\text{m}$. We have fitted the ‘8.1 μm ’ feature with 3 gaussians (see Fig. 5a,b and Table 2). We note from Table 2 that the widths of the features are typically $\sim 0.3 - 0.6 \mu\text{m}$, and so these are unlikely to be nebular in origin. Also listed in Table 2 are the ‘standard’ wavelengths and likely identification of ‘Class A’ UIR features (i.e. those usually seen in planetary nebulae and H II regions) from Geballe (1997).

There is no evidence that the central wavelengths of the two ‘shoulder’ features ($\sim 8.72 \mu\text{m}$, $\sim 9.20 \mu\text{m}$) change between Epochs 1 and 2; however there seems to be a distinct change in the peak wavelength of the primary feature between Epochs 1 and 2 (see Fig. 4a and Table 2), from 8.17 μm to 8.06 μm . This is not an artefact of the subtraction of the model from the data, and likely points to a change in the character of the carrier.

As noted in Paper II, the 11.3 μm feature in V705 Cas appears at a longer wavelength than is usual (the slight difference between the values in Table 2 and in Paper II is a result of the slight difference in the subtracted continuum). We note that there seems to be a significant increase in the strength of the 11.3 μm feature relative to that of the ‘8.1’ feature.

4.6.3 Why are nova UIR features unique?

It is of interest to consider why nova UIR features are in a class of their own (Geballe 1997), and in particular are significantly different from those seen in other astrophysical environments.

Laboratory measurements have shown that the peak wavelengths of the ‘3.28’, ‘6.2’, ‘7.7’, ‘8.1’ and ‘11.3’ UIR features in quenched carbonaceous composite depend on the $^{13}\text{C}/^{12}\text{C}$ ratio, the peak wavelengths increasing linearly with the $^{13}\text{C}/^{12}\text{C}$ ratio (Wada et al. 2003). However there are two reasons why this mechanism can not be operating in V705 Cas. First, the $^{13}\text{C}/^{12}\text{C}$ ratio in V705 Cas was low, $\lesssim 0.2$ (Paper I), so isotopic effects will have negligible effect on the wavelengths of the UIR features; however this effect must clearly be looked for in novae with high $^{13}\text{C}/^{12}\text{C}$ ratio. Second, the peak wavelengths of the nova 3.28 and 3.4 features are not anomalous, only their relative strengths are unusual. If isotopic effects were important the peak wavelengths of all the UIR features would be affected, which was not the case in V705 Cas.

More plausibly, the nature of the UIR carrier in novae is governed by the unique environment in which the pre-dust and dust chemistry takes place. We consider separately the UIR features in the 3 μm and 7-13 μm windows.

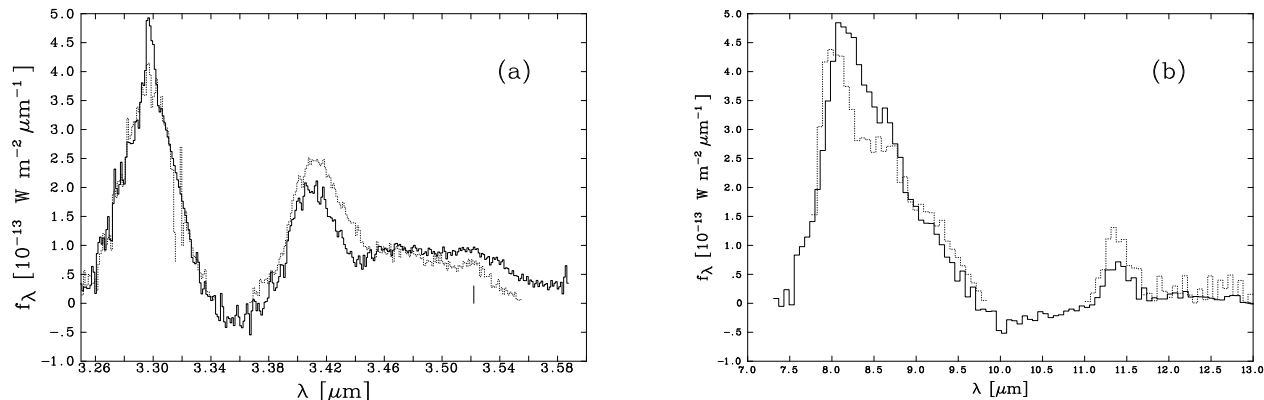


Figure 4. The profiles of the UIR features in V705 Cas; solid line, Epoch 1, broken line, Epoch 2. (a) The L -band features; the tick mark indicates the feature at $3.522 \mu\text{m}$ (see text). (b) the N -band features. Note the shift in wavelength of the $8 \mu\text{m}$ feature. See text for details.

Table 2. Properties of the UIR features in the N -band.

Epoch	λ (μm)	FWHM (μm)	Flux ($10^{-14} \text{ W m}^{-2}$)	Identification	Standard λ (μm) for Class A UIRs
1	8.17 ± 0.01	0.63 ± 0.03	$32.1 (\pm 1.4)$	Si-CH ₃ vibration?	...
	8.72 ± 0.02	0.41 ± 0.03	$10.8 (\pm 8.1)$	NH ₂ rock?	...
	9.20 ± 0.02	0.46 ± 0.04	$6.27 (\pm 0.43)$?	...
	11.41 ± 0.04	0.34 ± 0.08	$2.53 (\pm 0.51)$	Aromatic C-H bend	11.3
2	8.06 ± 0.06	0.47 ± 0.21	$7.27 (\pm 2.46)$	Si-CH ₃ vibration?	...
	8.67 ± 0.08	0.53 ± 0.20	$4.86 (\pm 1.89)$	NH ₂ rock?	...
	9.26 ± 0.15	0.52 ± 0.24	$2.34 (\pm 1.29)$?	...
	11.39 ± 0.12	0.38 ± 0.19	$1.51 (\pm 1.14)$	Aromatic C-H bend	11.3

4.6.3.1 The $3 \mu\text{m}$ window. As is well known, the relative strengths of the ‘3.28’ and ‘3.4’ features in novae differ substantially from those in other sources such as planetary nebulae and post-AGB stars (see e.g. Geballe 1997, van Dierhoven et al. 2004). A possible explanation for this is the incorporation of CH₂ and CH₃ groups in the silicate lattice, which experimental studies (Grishko & Duley 2002a) have shown enhances the $3.4 \mu\text{m}$ UIR feature.

As noted in §4.5, one explanation for the chemical dichotomy in nova dust shells is that CO does not proceed to saturation, allowing the simultaneous condensation of carbonaceous and silicate dusts: the chemistry of grain formation and growth is likely to include the formation of carbonaceous grains with silicate inclusions, and vice versa. The incorporation of CH₂/CH₃ groups into the silicate lattice in this way is consistent with the simultaneous presence of C-bearing and Si/O-bearing dust, and underlines the irrelevance of the C:O ratio to the nature of the condensate in nova winds.

Furthermore, (see §4.4), the grain size distribution indicates that larger grains may have swept up the smaller. Unless there were (for example) substantial species-dependent grain charge effects it is unlikely that larger grains would discriminate between one grain type and another in the sweeping-up process; this would also give rise to the kind of composite grain hinted at by the $3 \mu\text{m}$ UIR features.

4.6.3.2 The $7\text{--}13 \mu\text{m}$ window. Additional support for the hypothesis that CH₂/CH₃ inclusions in silicates could be significant in novae comes from the ‘8.1’ feature in V705 Cas. A feature at this wavelength is also seen in laboratory spectra, and may be identified with Si-CH₃ vibration (W. W. Duley, private communication). Indeed Duley (private communication) has suggested that the shift in the peak wavelength of the ‘8.1’ feature in V705 Cas between Epochs 1 and 2 (see Fig. 4 and Table 2) may be the result of a change in the co-ordination of Si-CH₃ groups.

Furthermore, it is likely that the UIR carrier in V705 Cas (and indeed in other novae) is heavily contaminated by other species, notably O or N, particularly the latter given its extreme overabundance (~ 100 ; see summary in Gehrz et al., 1998) relative to solar in nova winds. Grishko & Duley (2002b) have investigated experimentally the IR spectra of HAC prepared in the presence of various contaminants, and find that HAC deposited in the presence of N-bearing molecules (particularly NH₃) displays several features not present in ‘normal’ UIR carriers. In particular, there is a feature at $8.56 \mu\text{m}$ (which Grishko & Duley attribute to NH₂ rock), and a broad (unidentified) feature centred at $\sim 9.1 \mu\text{m}$ with width $\sim 0.4 \mu\text{m}$, which are close to the features on the ‘shoulder’ of the $8.1 \mu\text{m}$ feature in V705 Cas (see Fig. 5a,b and Table 2). We tentatively suggest that the carrier of the UIR features in V705 Cas had a significant nitrogen component.

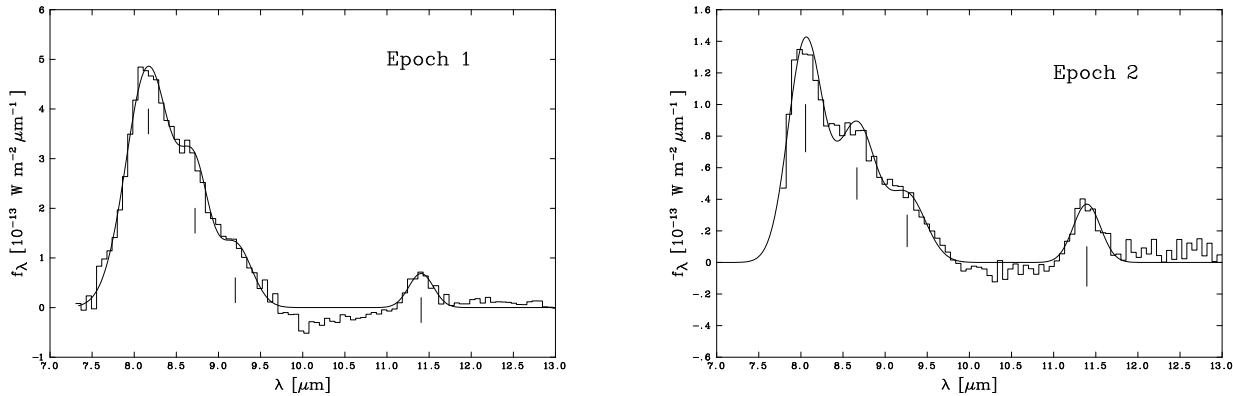


Figure 5. The profiles of the 7-13 μm UIR features in V705 Cas for Epoch 1 (left) and Epoch 2 (right). Curves are fitted gaussians; ticks marks locate peaks of individual features. See also Table 2.

5 CONCLUSIONS

We have used the *DUSTY* code to reassess the properties of the optically thick dust shell around the classical nova V705 Cas. We find

- (i) the dust shell is a $\sim 2 : 1$ (by number) mix of amorphous carbon and ‘warm silicate’;
- (ii) the grain size distribution $n(a) da \propto a^{-q} da$ was flat, with $q \simeq 2.3$; this may indicate that the larger grains swept up the smaller grains;
- (iii) the maximum grain size in the distribution was $a_{\text{max}} \simeq 0.06 \mu\text{m}$, considerably less than that deduced from previous studies (Shore et al. 1994, Paper II, Gehrz et al. 1998);
- (iv) the dust-bearing shell was, like the CO-bearing shell, geometrically thin, such that $\Delta R/R \simeq 0.1$;
- (v) the condensation temperature of the dust was $\sim 1100 \text{ K}$, although in V705 Cas the situation is complicated by the presence of two condensates;
- (vi) structure in the 8-9 μm UIR complex may be due to nitrogenation of the UIR carrier;
- (vii) the strength of the 3.4 μm feature relative to the 3.28 μm feature, commonly seen in novae, as well as the 8.1 μm feature, may be due to the incorporation of CH_2 and CH_3 groups in the silicate matrix;
- (viii) the silicate dust at least was freshly condensed, judging by the weakness of the 18 μm silicate feature;
- (ix) the extrapolated angular diameter of the dust shell is such that the resolved remnant seen by Diaz et al. (2001) was very likely due to line emission rather than dust.

ACKNOWLEDGMENTS

We thank Profs W. Duley and R. Gehrz for commenting on an early draft of this paper. TRG is supported by the Gemini Observatory, which is operated by the Association of Universities for Research in Astronomy, Inc., on behalf of the international Gemini partnership of Argentina, Australia, Brazil, Canada, Chile, the United Kingdom, and the United States of America. SPSE acknowledges support from the Nuffield Foundation. VHT was supported by Keele University.

REFERENCES

- Bath G. T., Shaviv G., 1976, *MNRAS*, 175, 305
 Beck H. K. B., Hauschildt P. H., Gail H.-P., Sedlmayr E., 1995, *A&A*, 294, 95
 Bouwman J., Meeus G., de Koter A., Hony S., Dominik C., Waters L. B. F. M., 2001, *A&A*, 375, 950
 Della Valle M., Livio M., 1995, *ApJ*, 452, 704
 Diaz M. P., Costa R. D. D., Jatenco-Pereira V., 2001, *PASP*, 113, 1554
 Evans A., Rawlings J. M. C., 1994, *MNRAS*, 269, 427
 Evans A., Geballe T. R., Rawlings J. M. C., Scott A. D., 1996, *MNRAS*, 282, 1049 (Paper I)
 Evans A., Geballe T. R., Rawlings J. M. C., Eyres S. P. S., Davies J. K., 1997, *MNRAS*, 292, 204 (Paper II)
 Evans A., Smith O., Tyne V. H., Rawlings J. M. C., Geballe T. R., Eyres S. P. S., 2002, in *Classical Nova Explosions*, Eds, M. Hernanz, J. José, AIP Conference Proceedings 637, p. 275
 Evans A., et al., 2003, *AJ*, 126, 1981
 Geballe T. R., 1997, In *From Stardust to Planetesimals*, ASP Conference Series, eds. Y. J. Pendleton, A. G. G. M. Tielens, Vol. 122, p. 119
 Gehrz R. D., Hackwell J. A., Grasdalen G. L., Ney E. P., Neugebauer G., Sellgren K., 1980, *ApJ*, 239, 570
 Gehrz R. D., Greenhouse M. A., Hayward T. L., Houck J. R., Mason C. G., Woodward C. E., 1995, *ApJ*, 448, L119
 Gehrz R. D., Truran J. W., Williams R. E., Starrfield S., 1998, *PASP*, 110, 3
 Gilman R. C., 1974, *ApJS*, 28, 397
 Grishko V. I., Duley W. W., 2002a, *ApJ*, 568, L131
 Grishko V. I., Duley W. W., 2002b, *ApJ*, 568, 448
 Hanner M. S., 1988, NASA Conference Publication 3004, p. 22
 Hauschildt P. H., Starrfield S. G., Shore S. N., Gonzalez-Riestra R., Sonneborn G., Allard F., 1994, *AJ*, 108, 1008
 Hauschildt P. H., Schwarz G., Short C. I., Baron E., Starrfield S., 2002, in *Classical Nova Explosions*, Eds, M. Hernanz, J. José, AIP Conference Proceedings 637, p. 249
 Hellyer B., 1970, *MNRAS*, 148, 383
 Ivezić Ž., Elitzur M., 1997, *MNRAS*, 287, 799
 Ivezić Ž., Nenkova M., Elitzur M., 1999, User Manual for *DUSTY*, University of Kentucky Internal Report
 Jones A. P., Tielens A. G. G. M., Hollenbach D. J., 1996, *ApJ*, 469, 740
 Kwok S., 1983, *MNRAS*, 202, 1149
 Mason C. G., Gehrz R. D., Woodward C. E., Smilowitz J. B., Hayward T. L., Houck J. R., 1998, *ApJ*, 494, 783
 Meeus G., Waters L. B. F. M., Bouwman J., van den Ancker M.

- E., Waelkens C., Malfait K., 2001, *A&A*, 365, 476
- Mitchell R. M., Evans, A., Bode M. F., 1983, *MNRAS*, 205, 1141
- Mitchell R. M., Evans, A., 1984, *MNRAS*, 209, 945
- Mitchell R. M., Evans, A., Albinson J. S., 1986, *MNRAS*, 221, 663
- Nuth J. A., Hecht J. H., 1990, *ApSpSci.*, 163, 79
- Orio M., Covington J., Ögelman H., 2001, *A&A*, 373, 542
- Ossenkopf V., Henning Th., Mathis J. S., 1992, *A&A*, 261, 567
- Pontefract M., Rawlings J. M. C., 2004, *MNRAS*, 347, 1294
- Press W. H., Teukolsky S. A., Vetterling W. T., Flannery B. P., 1992, *Numerical Recipes in Fortran*, Cambridge University Press
- Rawlings J. M. C., Evans A., 2005, *MNRAS*, to be submitted
- Rudy R. J., Lynch D. K., Mazuk S., Venturini C. C., Puetter R. C., Perry R. B., 2003, *BAAS*, 34, 1162
- Salama A., Eyres S. P. S., Evans A., Geballe, T. R., Rawlings J. M. C., 1999, *MNRAS*, 340, L20 (Paper III)
- Shore S. N., Gehrz, R. D., 2004, *A&A*, 417, 695
- Shore S. N., Starrfield S., Gonzalez-Riestra R., Hauschildt P. H., Sonneborn G., 1994, *Nature*, 369, 539
- Smith C. H., Aitken D. K., Roche P. F., Wright C. M., 1995, *MNRAS*, 277, 259
- Spitzer L., 1978, *Physics of the Interstellar Medium*, Wiley, New York
- Tielens A. G. G. M., Waters L. B. F. M., Molster F. J., Justtanont K., 1997, *ApSpSci*, 255, 415
- Tyne V. H., Evans A., Geballe T. R., Eyres S. P. S., Smalley B., Dürbeck H. W., 2002, *MNRAS*, 334, 875
- van Dienenhoven B., Peeters E., Van Kerckhoven C., Hony, S., Hudgins D. M., Allamandola L. J., Tielens A. G. G. M., 2004, *ApJ*, 611, 928
- Wada S., Onaka T., Yamamura I., Murata Y., Tokunaga A. T., 2003, *A&A*, 407, 551
- Warner B., 1995, *Cataclysmic Variable Stars*, Cambridge University Press
- Werner M. W., et al., 2004, *ApJS*, 154, 1
- Woodward C. E., Greenhouse M. A., 1993, *IAUC5910*
- Zijlstra A. A., Chapman J. M., te Linkel Hekkert P, Likkel L., Comeron F., Norris R. P., Molster F. J., Cohen R. J., 2001, *MNRAS*, 322, 280

This paper has been typeset from a \TeX / \LaTeX file prepared by the author.

